16p

(TMX-54525)

EXPERIMENTAL INVESTIGATION OF SIMULATED SPACE PARTICULATE RADIATION EFFECTS ON MICROELECTRONICS

Emanuel Rind and Floyd R. Bryant [1964] 16p refs

1608751

NASA, Langley Research Center
Langley Station, Hampton, Va.

Presented at the 1964 IEEE International Convention

☐ Conf.

New York, N.Y.
March 23-26, 1964

Unc.

[redacted]

EXPERIMENTAL INVESTIGATION OF SIMULATED SPACE PARTICULATE RADIATION EFFECTS ON MICROELECTRONICS

Emanuel Rind and Floyd R. Bryant
Aerospace Technologists, Radiation Effects Instrumentation Section
Instrument Research Division
NASA Langley Research Center

SUMMARY

35208/A

Microelectronics, like their more conventional solid-state counterparts, are adversely affected by radiation environments such as those found in outer space. These space radiation environments are briefly summarized. Proton irradiation data at 22, 40, 128, and 440 Mev are presented for typical macroelectronic components such as low-, medium-, and high-frequency transistors and compared with similarly irradiated discrete- and integrated-circuit type of microcomponents. Damage tends to vary inversely with energy. Integrated flux levels of approximately 10^{11} protons/cm^2 are needed before the radiation effects become noticeable. Integrated circuits appear to be slightly more resistant to radiation but this finding may not be significant on a statistical basis. A typical experimental setup and circuit which were actually used in the tests are illustrated and described.

INTRODUCTION

Author

The inherent advantage of microelectronics with their compactness, low weight, ruggedness, and ability to be formed into reliable, complex circuitry has resulted in their increased application in space missions. However, one aspect of the space environment to which conventional solid-state electronic systems have shown themselves to be especially sensitive is the particulate radiation that (1) is found in the radiation belts, (2) is generated by solar flares, (3) is a result of detonations of manmade nuclear and atomic devices, or (4) is of cosmic origin.

SYMBOLS

A	direct-current voltage gain
E	energy
$f_{\alpha b}$	frequency at which magnitude of small-signal short-circuit forward-current transfer ratio is 0.707 of its low frequency value
g_m	transconductance
h_{FE}	common emitter, static value of short-circuit forward-current transfer ratio, I_C/I_B
h_{fe}	common emitter, small-signal forward-current transfer ratio, alternating-current output short-circuited, $\Delta i_c/\Delta i_b$
I_B	direct current into base
I_C	direct current into collector
I_{CBO}	collector to base current, emitter open
L	distance in earth radii
R_{DP}	displacement rate
R_L	load resistance
V_{CE}	voltage, collector to emitter
V_{DS}	voltage, drain to source
BV_{CBO}	voltage, breakdown, collector to base
Φ_t	total integrated flux

Subscript:

o	initial conditions

NOTATIONS

Ge	germanium
Si	silicon

SUMMARY OF THE SPACE PARTICULATE ENERGY ENVIRONMENT

The current knowledge of the flux and energy levels of particulate energy in space is summarized in table I (refs. 1 and 2).

The proton data of table I do not imply that the energy spectrum is nonexistent between 4.5 and 30 Mev. This gap exists because of the limitations of the detectors which were used, and the data are therefore not available. Solar activity can cause an increase in the trapped proton intensities but their contribution to any discrete energy is time dependent. The flare spectra with time generally shifts toward the lower energies for initial energies >80 Mev and toward the higher energies for initial energies <80 Mev. Thus the intensities at energies <80 Mev increase at the expense of reduced intensities in the higher energy range. Increases of belt proton intensity by factors of 2 or 3 have been reported during solar activity especially in the low-energy part of the spectrum observed down to at least 8 Mev (ref. 3). Winckler and Arnoldy (ref. 4) feel that the observed counting rate increases do not unambiguously mean that the intensity of the trapped high-energy proton radiation has increased but rather could be the result of a small shift in the spectrum such that more particles fall into the energy range above the cutoff of the detector (30 Mev).

The low-energy protons populate the region between 3.1 and 4.7 earth radii, whereas the high-energy protons are encountered at about 1.6 earth radii.

Solar flares produce protons with energies extending to about 10 Bev but these have very low fluxes. The maximum integral energy flux varies between 10^5 and 10^6 protons/cm^2/sec, with the largest number of these having energies less than 700 Mev (refs. 5 and 6). As has been noted, these spectra change with time.

[redacted]

The highest integrated intensities of the natural belt electrons are between 10^8 and 10^9 electrons/cm^2/sec and lie between 2.5 and 4.2 earth radii with a corresponding energy range from tens of Kevs to approximately 1.6 Mev. The energies of the trapped electrons exceed 5 Mev and may go as high as 10 Mev.

A high-altitude nuclear detonation in 1962 produced a manmade belt of electrons at about 1.65 earth radii with peak integrated intensities greater than 10^9 electrons/cm^2/sec, the greatest contribution being at about 1 Mev. The energies of the manmade electrons extend from a few thousand electron volts to about 7 Mev. The intensity >7 Mev approaches zero. The spectra for these belts can be found in reference 7. The intensities of these belts have been slowly diminishing with time and the peak integrated electron intensities reported from Explorer XV data were approximately 5×10^8 electrons/cm^2/sec > 0.5 Mev at $L = 1.3$ and approximately 1.9×10^7 electrons/cm^2/sec > 5.0 Mev at $L = 1.3$ (ref. 8). This same reference states that, "The time constants for change by a factor of e (=2.718) in this region are typically greater than 1 year and in many cases appear greater than 3 years. Should these electrons injected by the "Starfish" detonation continue to decay at the observed rates, it will be possible to detect their presence among the naturally dropped particles for at least 20 years."

EXPERIMENTAL RESULTS FROM IRRADIATED ELECTRONIC DEVICES

Conventional Electronics

The experimental data presented herein were obtained using several proton accelerators of different energies. The effects of particulate radiation on conventional solid-state components are shown in figures 1 and 2 and will be used for a comparison with the effects of 40 Mev protons on the small-signal current gain of thin-base-region, medium-base-region, and thick-base-region resistors which correspond to high-, medium-, and low-frequency transistors, respectively. (See ref. 9.) It is readily apparent that though all three types of transistors show degradation of gain with increasing flux, the least degradation occurs in those components having thin-base regions. At an integrated flux of 10^{12} protons/cm^2, the gain of the high-frequency transistor is degraded approximately 10 percent, whereas the low-frequency transistor is degraded approximately 80 percent.

The energy dependence of small-signal current-gain degradation is shown in figure 2. All other parameters being equal, it has been found that higher degradations occur for lower incident particle energies. Theory indicates that permanent radiation damage is predominantly caused by lattice displacements. The displacements, in turn, produce interstitial-vacancy pairs which result in recombination or trapping centers. Since threshold energies for displacements are approximately 8,000 ev times the atomic weight for electrons and 7 ev times the atomic weight for protons, relatively low energies will produce displacements. (See ref. 10.) As the incident particle energy increases, the cross section for displacements decreases and inelastic and transmutation processes become more predominant for producing permanent damage, as shown in figure 3. Roughly, for protons below 8 Mev, Rutherford scattering will acount for most of the damage; up to 50 Mev, Rutherford plus nuclear elastic scattering processes are involved; and above 50 Mev, inelastic and higher order processes should be included. (See ref. 11.) As the higher energy processes produce effects which are about two orders of magnitude less than the low-energy processes, less degradation should be expected with increasing incident particle energies in semiconductors.

The experimental data in figures 1 and 2 were obtained with the use of transistors in which the operation depended upon minority carriers. Figure 4 shows experimental data obtained from the majority-carrier field-effect transistor. Preir-radiation and postirradiation results are shown for 128 Mev protons. Drain current is plotted against gate voltage. If the gate voltage operating limit is considered to be between 0 and 0.6 volt, the degradation in drain current between the preirradiation and postirradiation values is approximately 30 percent. However, since the transconductance g_m is equal to the slope of the curves and the gain is approximately equal to the transconductance g_m times the load resistance R_L for low frequencies (where R_L is constant), gain degradation after irradiation amounts to only about 10 percent. Conductivity measurements made on boron-doped silicon subjected to similar proton irradiation have given results analogous to those obtained with the field-effect transistor when operated at zero gate voltage. Generally, majority-carrier devices which depend on resistivity are more radiation-resistant than minority-carrier devices which depend on minority-carrier lifetime.

Microminiature Electronics

Microminiature electronics concerns itself with electronic components of high packing density. These electronics may be divided into three main categories: (1) discrete conventional components of microminiature size, (2) thin-film components either printed or evaporated, and (3) integrated circuits, which have been defined as monolithic semiconductor substrates containing both active and passive devices and their interconnections, all of which have been either diffused into or deposited on the substrate surface in such a way as to produce within the substrate, complete functional electronic circuits.

At present, the state of the art of thin-film electronics has not produced electronic components or circuits with stable shelf life. (These devices are made with evaporated films under 1,500 angstroms thick.) For this reason, none of these devices are now being evaluated (ref. 12). Of the remaining two classes - integrated-circuit elements and discrete microminiature components - initial tests have been made by using 128 Mev protons at the Harvard frequency-modulated cyclotron and 22 Mev protons at the Oak Ridge National Laboratory fixed-frequency cyclotron. Typical data obtained from these irradiations are shown in figure 5 for a μET-1 (NPN Si) diffused silicon integrated-circuit transistor. Again, the higher energy protons produced less degradation in gain than the lower energy protons for the same integrated flux. In this limited sampling, however, the degradation takes place at slightly higher integrated flux values than those for conventional transistors. Once the degradation threshold is reached, degradation continues almost monotonically with flux. It may

be noted that data at 128 Mev were not carried to the same integrated fluxes as the lower energy because frequency-modulated cyclotrons have beam intensities approximately two orders of magnitude lower than fixed-frequency cyclotrons, and lack of available cyclotron time at 128 Mev did not permit extending the data. Actual preirradiation and postirradiation oscilloscope photographs of the common emitter collector characteristics for this microtransistor are shown in figures 6(a) and 6(b). The postirradiation photograph was taken when the total integrated bombarding flux of 128 Mev protons was at 6×10^{12} protons/cm^2. The average degradation produced by the irradiation caused a 30 percent reduction in collector current. Other integrated-circuit components, such as diffused silicon integrated-circuit resistors and diodes (type μER-1 and μED-1), were also irradiated at 128 and 22 Mev protons. Negligible adverse effects were obtained at integrated fluxes of 4.5×10^{12} protons/cm^2 at 128 Mev and greater than 10^{13} protons/cm^2 at 22 Mev. A type "F" flip-flop integrated circuit exposed to the radiation conditions just stated showed minimal effects in operation at 200 kilocycles. Other effects are presented in table II. None of the reduced values caused by irradiation made the circuit inoperative and, in the instance of the rise time changing from 0.100 μsec to approximately 0.030 μsec, there actually is an improvement which cannot be explained by us at this time.

Typical discrete microminiature electronic components, such as diffused silicon microdiodes, NPN silicon microtransistors, silicon microzener diodes, and planar double-diffused silicon NPN Darlington connected amplifiers, were irradiated with 128 Mev protons to a total integrated flux of 4.5×10^{12} protons/cm^2. The diodes after irradiation showed less than a 5-percent change in forward and reverse current as well as breakdown voltage. One of the microtransistors, a TMT-843, NPN-silicon type which received a total integrated flux of 1.5×10^{12} protons/cm^2 at 128 Mev, dropped to 80 percent of its initial direct-current gain. Figure 7 shows the gain degradation versus base current for this microtransistor. The Darlington connected amplifier, which is made by diffusing two direct-coupled transistors on one substrate, dropped to 23 percent of its original direct-current gain.

Table III shows some comparative values of integrated flux needed to produce equal degradation in conventional and microminiature electronic components.

The first three transistors are of the conventional low-, medium-, and high-frequency types of transistors. The flux tolerance between the low-frequency and high-frequency transistor is a factor of 10 favoring the high-frequency type. The integrated-circuit transistors are slightly more radiation-tolerant than the high-frequency conventional types and behave similarly to discrete microtransistors. The Darlington connected transistors, because of their configuration, become quite vulnerable to radiation as can be seen by their drop in gain to 30 percent of their original value at 5.6×10^{11} protons/cm^2. The field-effect transistors, which are majority carrier devices, appear to give the best radiation-resistant performance. The performance, however, is comparable with the radiation resistance of the microelectronic integrated-circuit transistors.

Description of Experimental Setup

A typical schematic drawing and photograph of the experimental setup as used at the Harvard 128 Mev and the ORNL 22 Mev proton accelerator facilities are shown in figures 8 and 9. Readout of all the pertinent parameters were made in the shielded control room. The microelements were individually fixed on an aluminum mounting plate which had been perforated to permit passage of the beam. The plate was set normal to the proton beam. Remotely controlled positioning motors drove the mounting plate in the normal plane thus positioning any desired microelement in the beam. A silver activated zinc sulphide phosphor positioned on the mounting plate was used to locate the beam center line. This position was marked on the screen of a closed-circuit television monitor. Each microelement was then positioned to the index on the TV screen. Beam drift was checked occasionally by use of the phosphor. An ion chamber placed between the beam exit port and mounting plate was calibrated with a Faraday cup and was used during the irradiation to monitor beam current. A current integrator was used for obtaining the integrated flux. A sixteen channel remote switching circuit was used for monitoring and activating any individual microelement. Bias voltage was kept on eight of the sixteen channels before and during all irradiations to determine whether there were any differences in results from this source. Measurements of h_{fe} and h_{FE} were made at various integrated flux values and BV_{CBO} and I_{CBO} measurements were made at the beginning and end of each test.

Figure 10 is a detailed circuit for the type "F" element used in the tests. The circuit simulates micrologic inputs and loads for the "F" element. With an applied 3-volt pulse or square wave, the input 2N743, representing preceding micrologic stages, generates 0.2 μsec, 1-volt pulses. Each of the output transistors with its base resistor represents one micrologic load. Generally, up to four such loads may be carried in parallel at each output.

FUTURE WORK

Very little proton and electron irradiation data on microelectronics exist. These devices like their conventional counterparts are sensitive to the space particulate radiation environment. Considerable data will have to be accumulated as these devices become available for determining reliability criteria in a radiation environment. This work, in conjunction with basic studies on their constituent materials, is presently in progress at the Langley Research Center and other laboratories and may lead to the elimination of space radiation as a problem in this particular area.

CONCLUDING REMARKS

Most of the existing information for proton and electron irradiation is on conventional or solid-state macroelectronic components. Because of the limited availability of accelerator time, even these data are not numerous. The information that does exist indicates that these components are radiation-sensitive and that for transistors 30-percent-gain degradation occurs at proton

integrated flux levels of approximately 10^{11} protons/cm^2. This value corresponds roughly to several days or months of belt or solar flare radiation, depending on the proton spectra encountered in the mission orbit. The present trend is to use solid-state microelectronic circuitry in future space-vehicle systems. Initial tests indicate that this type of circuitry is also radiation-sensitive and generally follows the same trends as the macrocomponents. However, with few exceptions, slightly higher integrated fluxes are required to produce similar degradation. This difference may not be significant in that a very small sampling was available for comparison and, on a statistical basis, it may disappear. Efforts will be made to obtain sufficient experimental data for establishing design and reliability criteria and for correlating the results with the experimental data being obtained at Langley Research Center on the basic materials which comprise these devices.

REFERENCES

1. T. Foelsche, "Radiation Doses in Interplanetary Flight," Paper presented at Ninth Annual American Astronautical Society Meeting of the Interplanetary Missions Conference, Los Angeles, Calif.; Jan. 15-17, 1963.

2. Frank B. McDonald, ed., "Solar Proton Manual," NASA TR R-169; 1963.

3. John E. Naugle and Donald A. Kniffen, "The Flux and Energy Spectra of the Protons in the Inner Van Allen Belt," NASA TN D-412; 1961.

4. J. R. Winckler and R. L. Arnoldy, "Energetic Particles in the Magnetosphere," NASA-CR-51177, TR CR-66; June 1963.

5. J. R. Winckler, "Primary Cosmic Rays," Proceedings of Conference on Radiation Problems in Manned Space Flight, Geo. J. Jacobs, ed., NASA TN D-588; 1960, pp. 72-93.

6. D. K. Bailey, "Abnormal Ionization in the Lower Ionosphere Associated With Cosmic-Ray Flux Enhancements," Proc. Inst. Radio Engineers, vol. 47, no. 2; Feb. 1959, pp. 255-266.

7. Wilmot N. Hess, "The Artificial Radiation Belt Made on July 9, 1962," NASA TN D-1687; April 1963.

8. C. E. McIlwain, "The Radiation Belts, Natural and Artificial," Science, vol. 142; Oct. 18, 1963, pp. 355-361.

9. W. C. Honaker and F. R. Bryant, "Irradiation Effects of 40 and 400 Mev Protons on Transistors," NASA TN D-1490; 1963.

10. L. D. Jaffe and J. B. Rittenhouse, "Behavior of Materials in Space Environments," TR 32-150 (Contract No. NASw-6), Jet Propulsion Lab., C.I.T.; Nov. 1, 1961.

11. D. M. Arnold, J. A. Baicker, et al., "Proton Damage in Semiconductor Devices," RCA (NASA Contract No. NASI-1654); Nov. 1, 1962.

12. Weimer, Paul K., "The TFT - A New Thin-Film Transistor," Proceedings of the IRE; June 1962, pp. 1462-1469 and private communication with the author.

TABLE I.- SUMMARY OF THE PROTONS AND ELECTRONS IN SPACE

Low energy	High energy
Radiation-belt protons	
120 Kev < E < 4.5 Mev Flux ≈ 10^8 protons/cm^2/sec	30 Mev < E < 700 Mev Flux ≈ 2×10^4 to 4×10^4 protons/cm^2/sec
Intensity can vary by a factor of 2 to 3 with solar activity	
Solar flares	
E < 40 Mev Flux ≈ 10^5 to 10^6 protons/cm^2/sec	E → 10 Bev
Electrons	
110 Kev < E < 1.6 Mev Flux < 10^8 electrons/cm^2/sec E > 10 Kev Flux ≈ 10^9 electrons/cm^2/sec	1.6 Mev < E < 5 Mev Flux < 10^5 electrons/cm^2/sec E > 5 Mev Flux < 10^3 electrons/cm^2/sec
Intensity can vary by a factor of 50 to 100 with solar activity	

TABLE II.- PROTON IRRADIATION OF A TYPE "F" LOGIC ELEMENT

FLIP-FLOP INTEGRATED CIRCUIT

Parameter	Preirradiation	Postirradiation
E = 128 Mev		
Positive output pulse width, μsec . . . Amplitude, volts . . . . . . Rise time, μsec	1 0.8 0.1	0.8 0.64 0.1
E = 22 Mev		
Positive output pulse width, μsec . . . Amplitude, volts . . . . . . Rise time, μsec	1 0.7 0.100	0.9 0.63 ≈0.030

TABLE III.- INTEGRATED PROTON FLUX VALUES FOR PRODUCING

30-PERCENT-GAIN DEGRADATION IN TRANSISTORS

Transistor type	Energy, Mev	Maximum tolerance flux, protons/cm^2	Nominal frequency, mc	Remarks
2N224 (PNP Ge)	40	1.5×10^{11}	0.5	
2N169 (NPN Ge)	40	7×10^{11}	9	
2N743 (NPN Si)	40	1.8×10^{12}	*400	
μET-1 (NPN Si)	128	4.5×10^{12} $\left(h_{FE}/h_{FE,o} = 0.78\right)$	------	Integrated-circuit transistor
	22	4.1×10^{12}	------	
TMT-843 (NPN Si)	128	1.4×10^{12} $\left(h_{FE}/h_{FE,o} = 0.81\right)$	20	Microtransistor
MHM 1101 (NPN Si)	128	5.6×10^{11} $\left(h_{FE}/h_{FE,o} = 0.27\right)$	60	Darlington connected
2N2497	128	3.36×10^{13} $\left(A/A_o = 0.87\right)$	------	Field-effect transistor
	22	5.34×10^{13} $\left(A/A_o = 0.74\right)$	------	
TIX-880	128	6.72×10^{12} $\left(A/A_o = 0.64\right)$	------	Field-effect transistor

*Frequency when $h_{FE} = 1.0$.

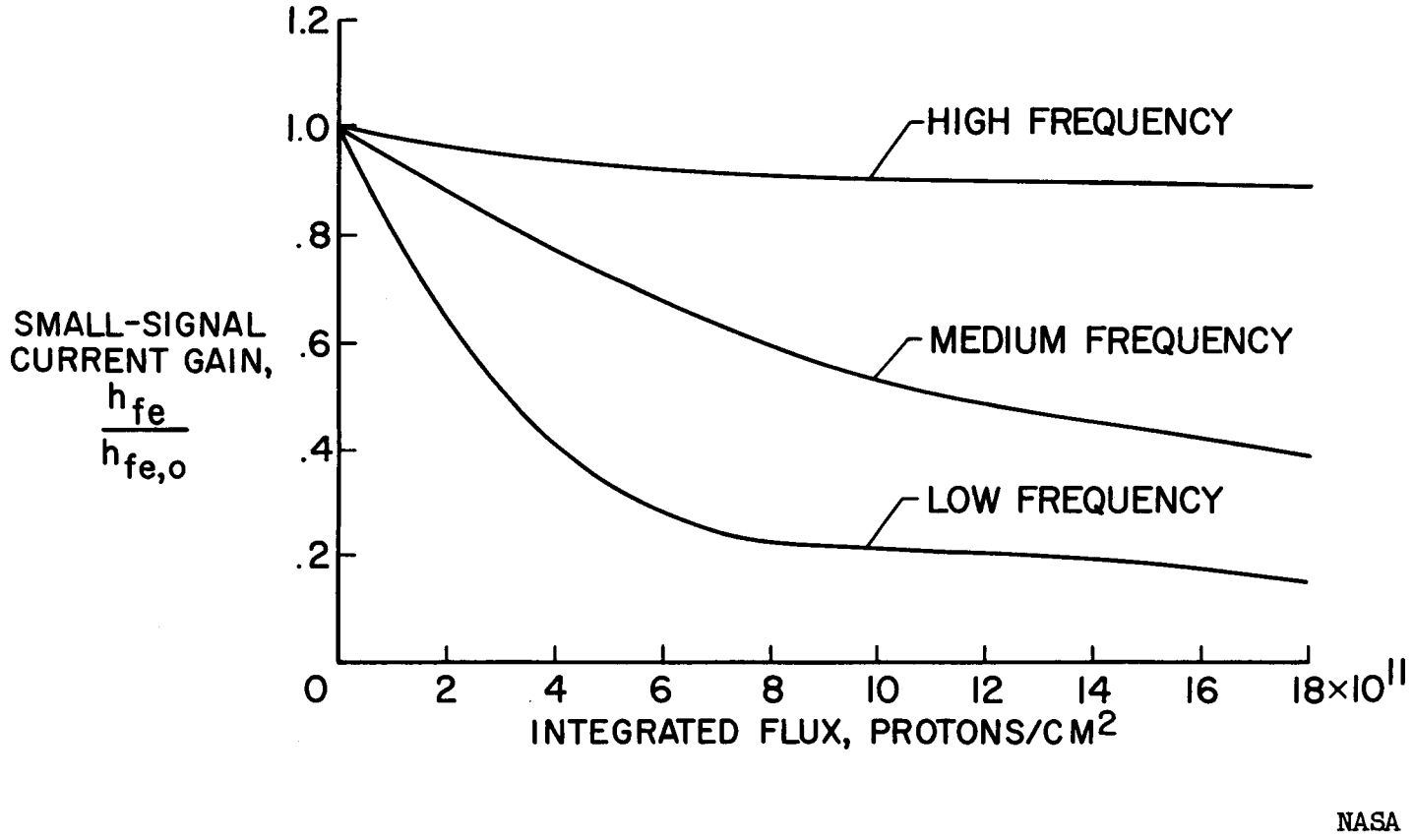

Figure 1.- Relative damage to transistors due to 40 Mev protons.

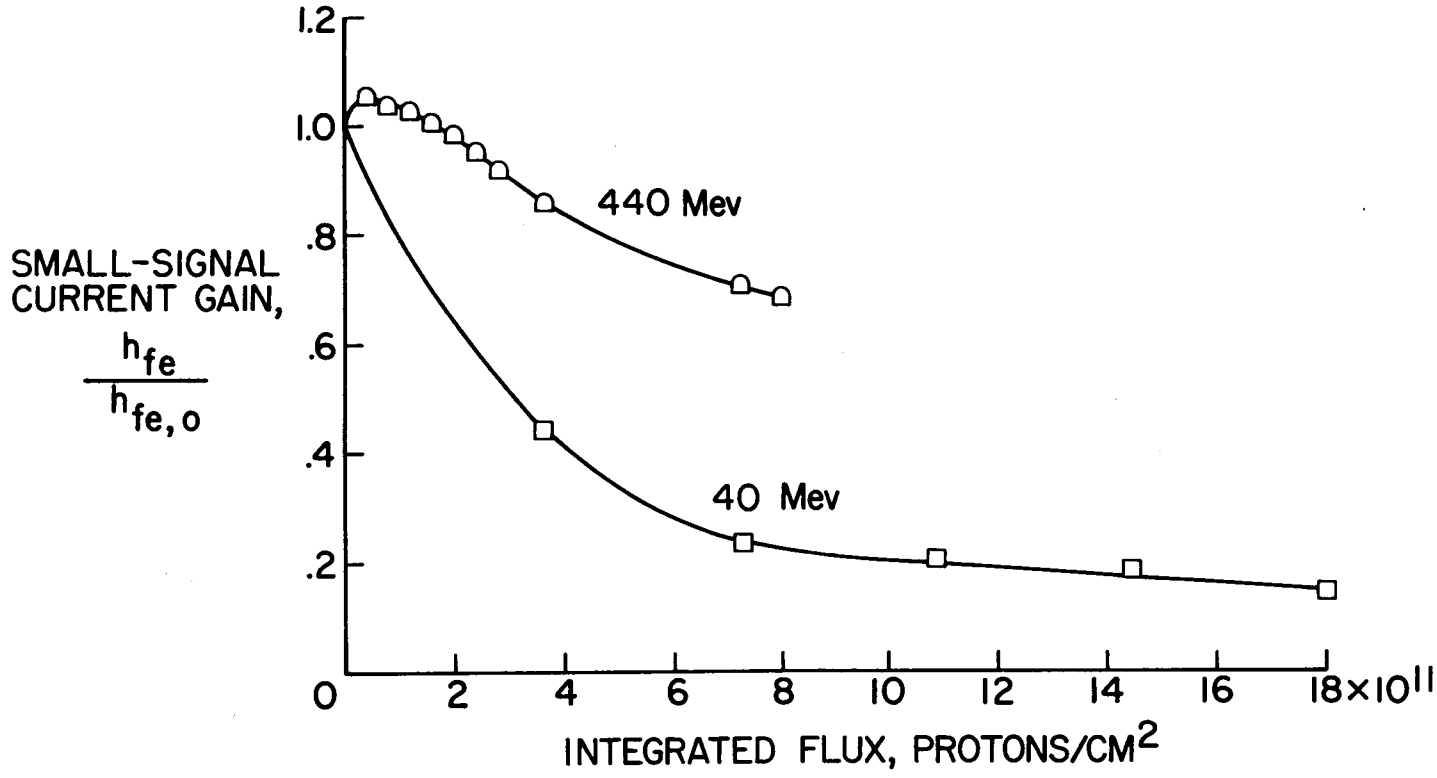

Transistor type 2N224; PNP Ge; alloy junction; $f_{\alpha b}$ = 0.5 mc. NASA

Figure 2.- Proton damage at two energies.

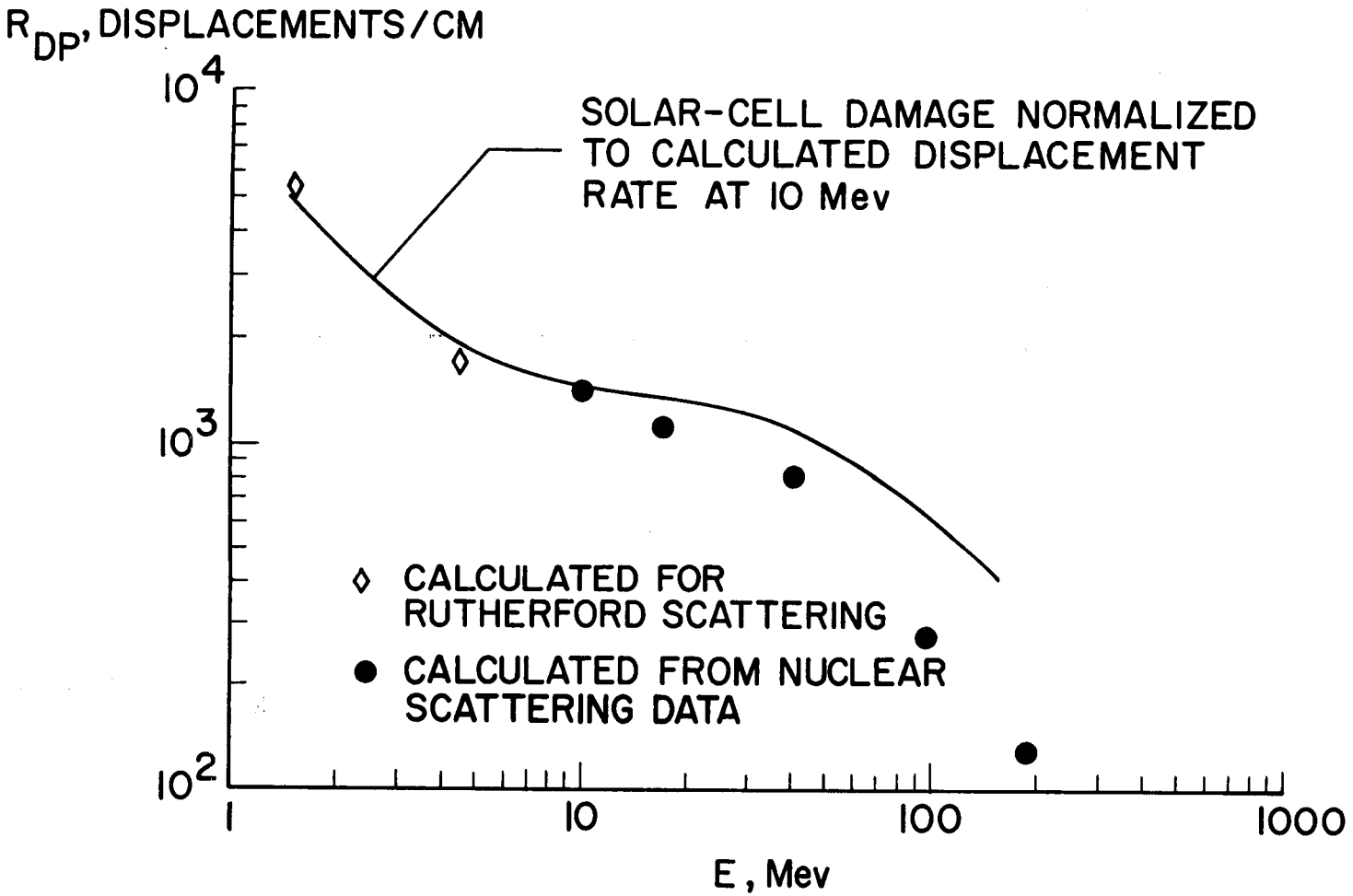

Figure 3.- Lattice displacements as a function of proton energy.

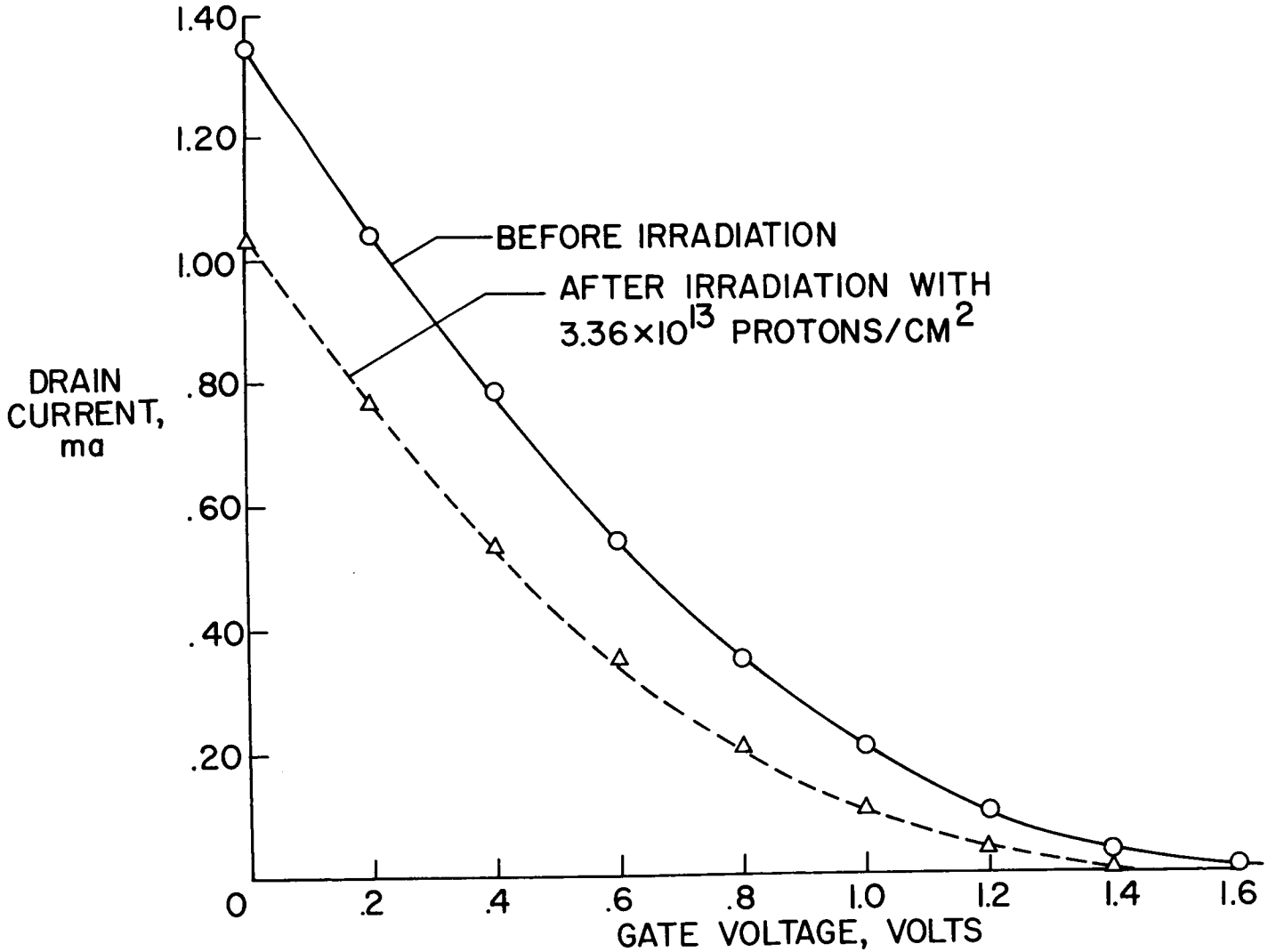

128 Mev protons; type 2N2497; P-channel silicon; V_{DS} = -10 volts. NASA

Figure 4.- Radiation effects on field-effect transistor.

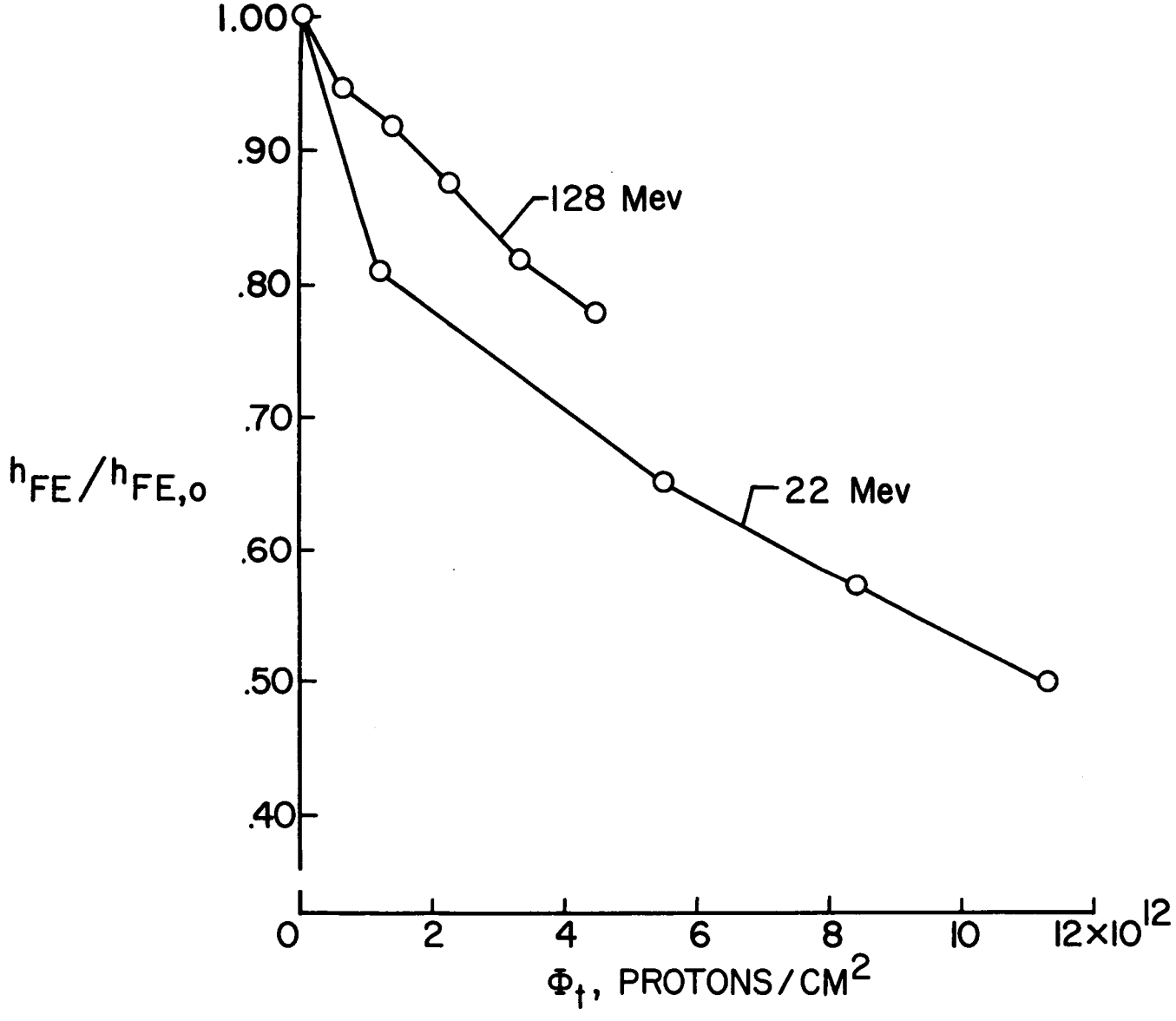

μET-1(NPN Si); V_{CE} = 4.5 v; I_B = 60 μa. NASA

Figure 5.- Direct-current gain as a function of proton flux.

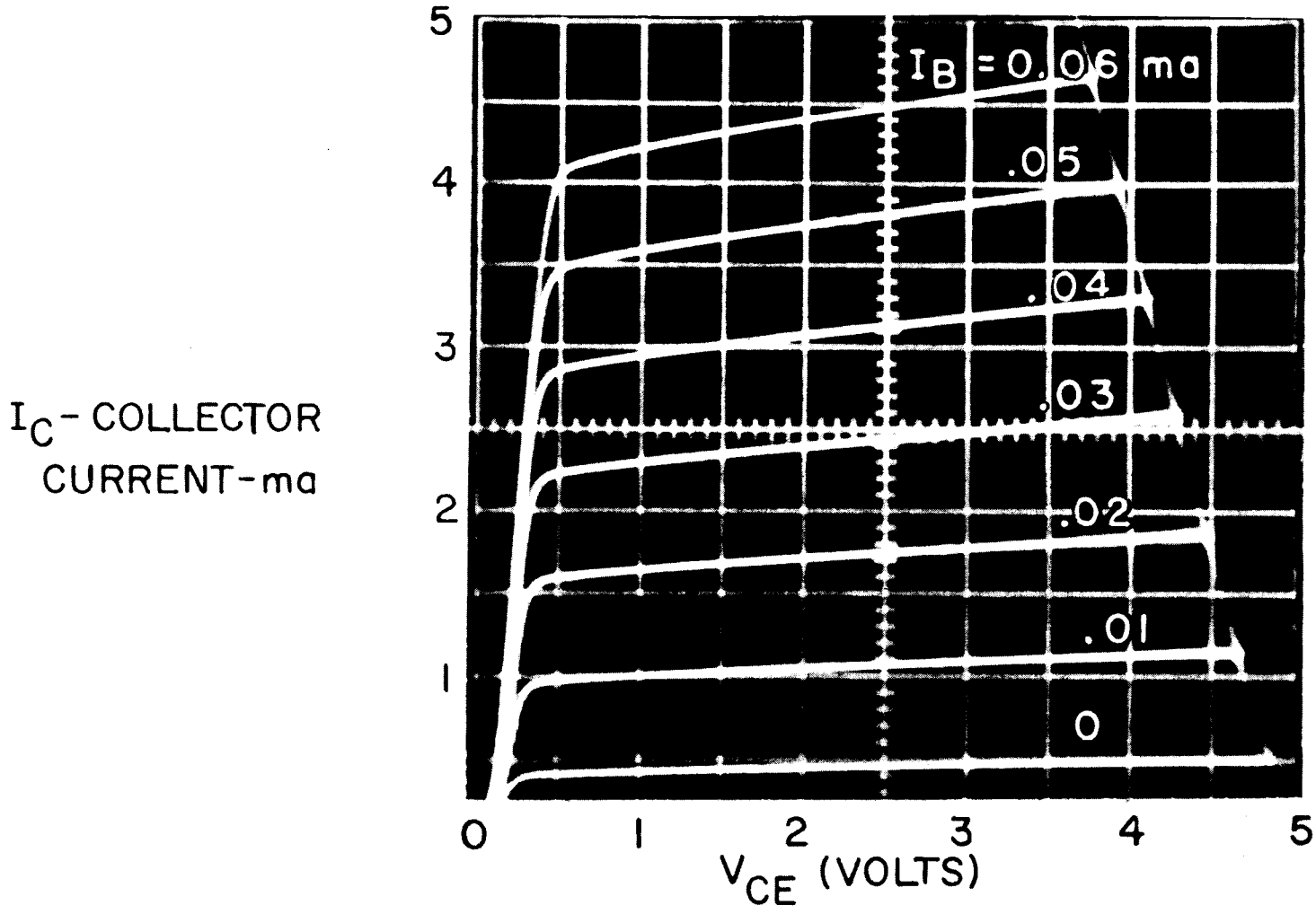

NASA

Figure 6(a).- Preirradiation common emitter collector characteristics of a planar type (μET-1, NPN-Si) diffused silicon integrated circuit transistor.

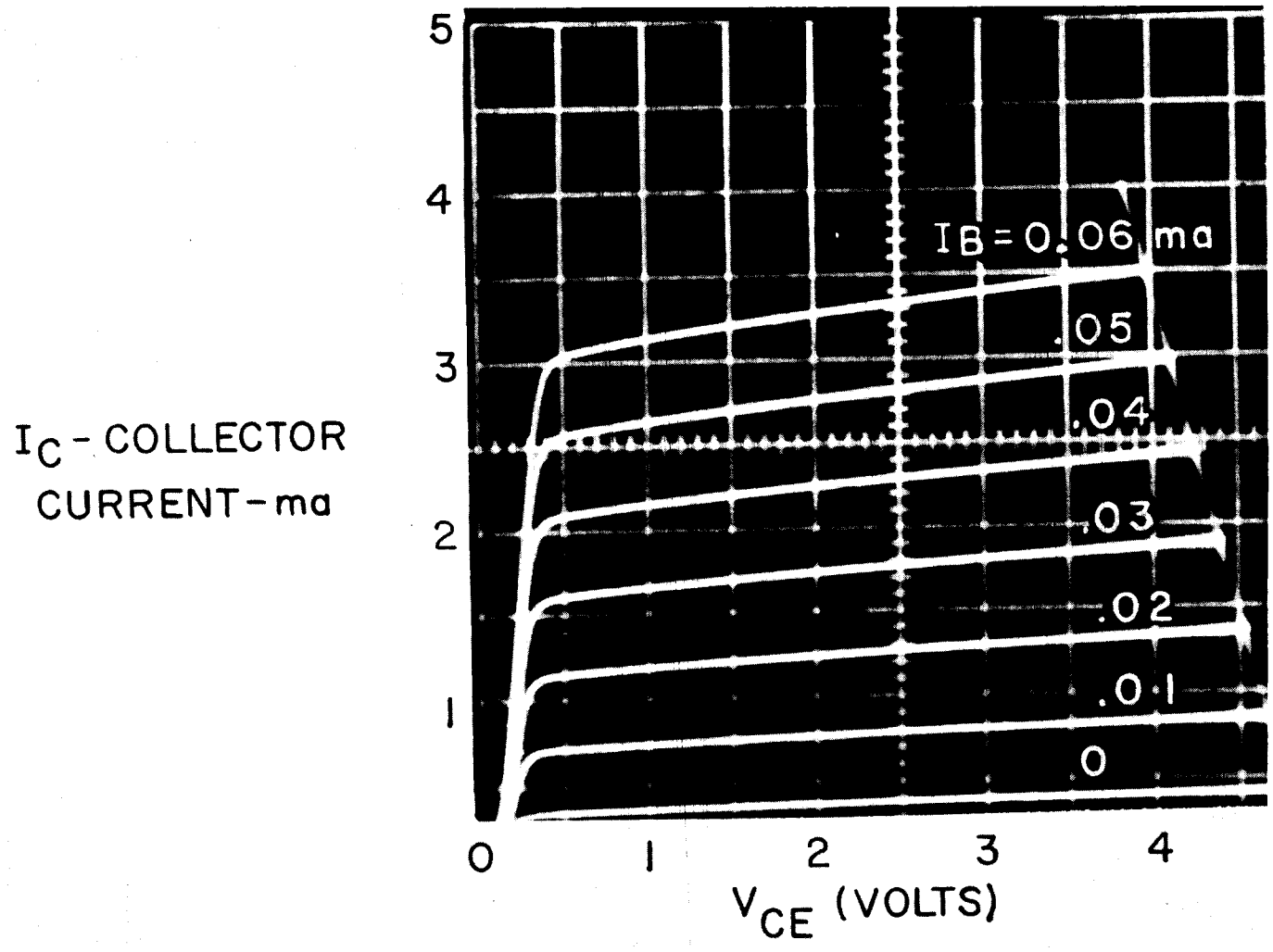

NASA

Figure 6(b).- Postirradiation common emitter collector characteristics of the integrated circuit transistor in figure 6(a). The transistor was bombarded with 128 Mev protons with an integrated flux of 6.25×10^{12} protons/cm^2.

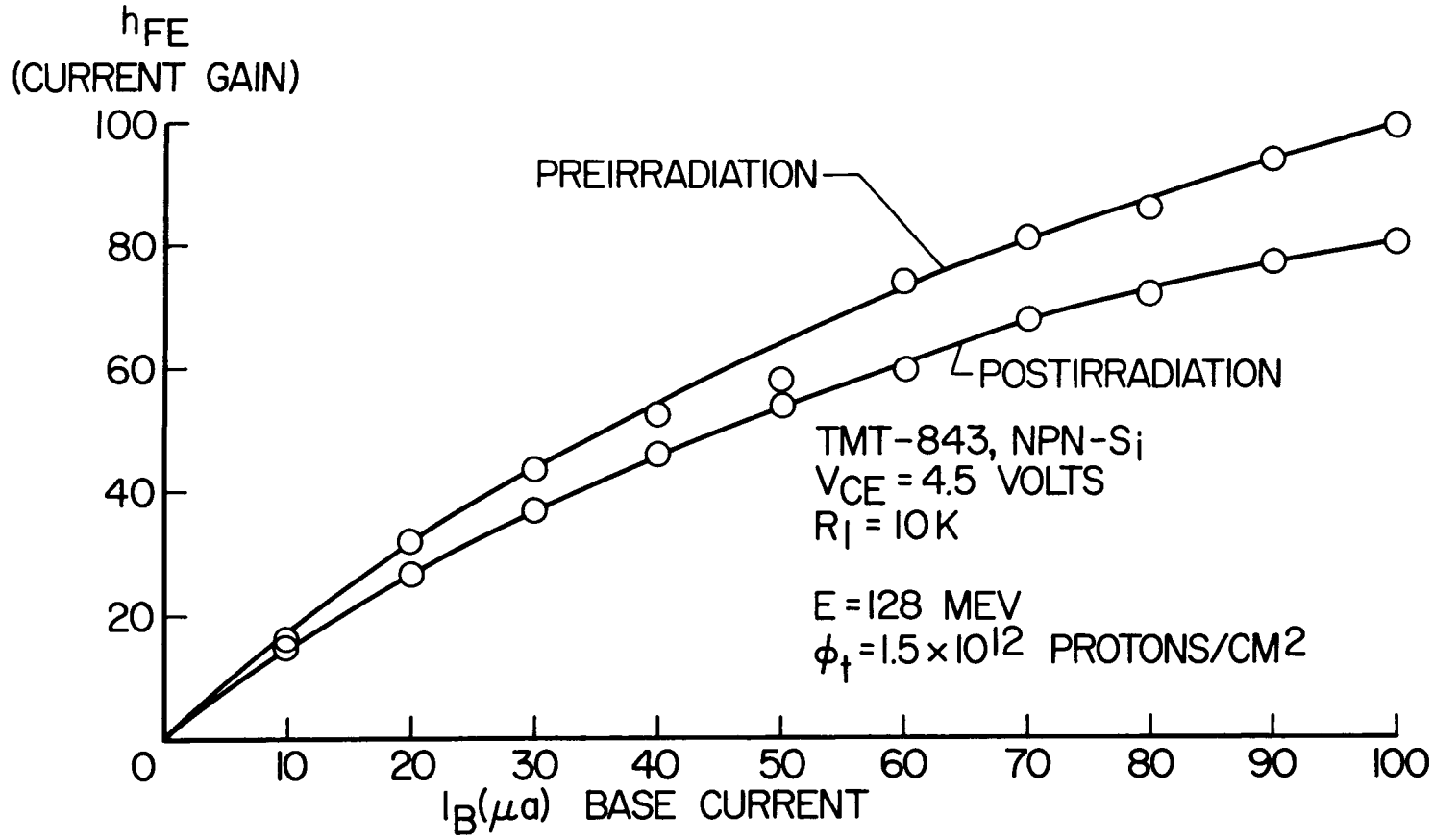

NASA

Figure 7.- Plots of the preirradiation and postirradiation direct current gain versus base current for a typical (TMT-843, NPN-Si) microtransistor. The transistor was bombarded with 128 Mev protons with an integrated flux of 1.5×10^{12} protons/cm^2. (V_{CE} = 4.5 volts, R_l = 10 KΩ.)

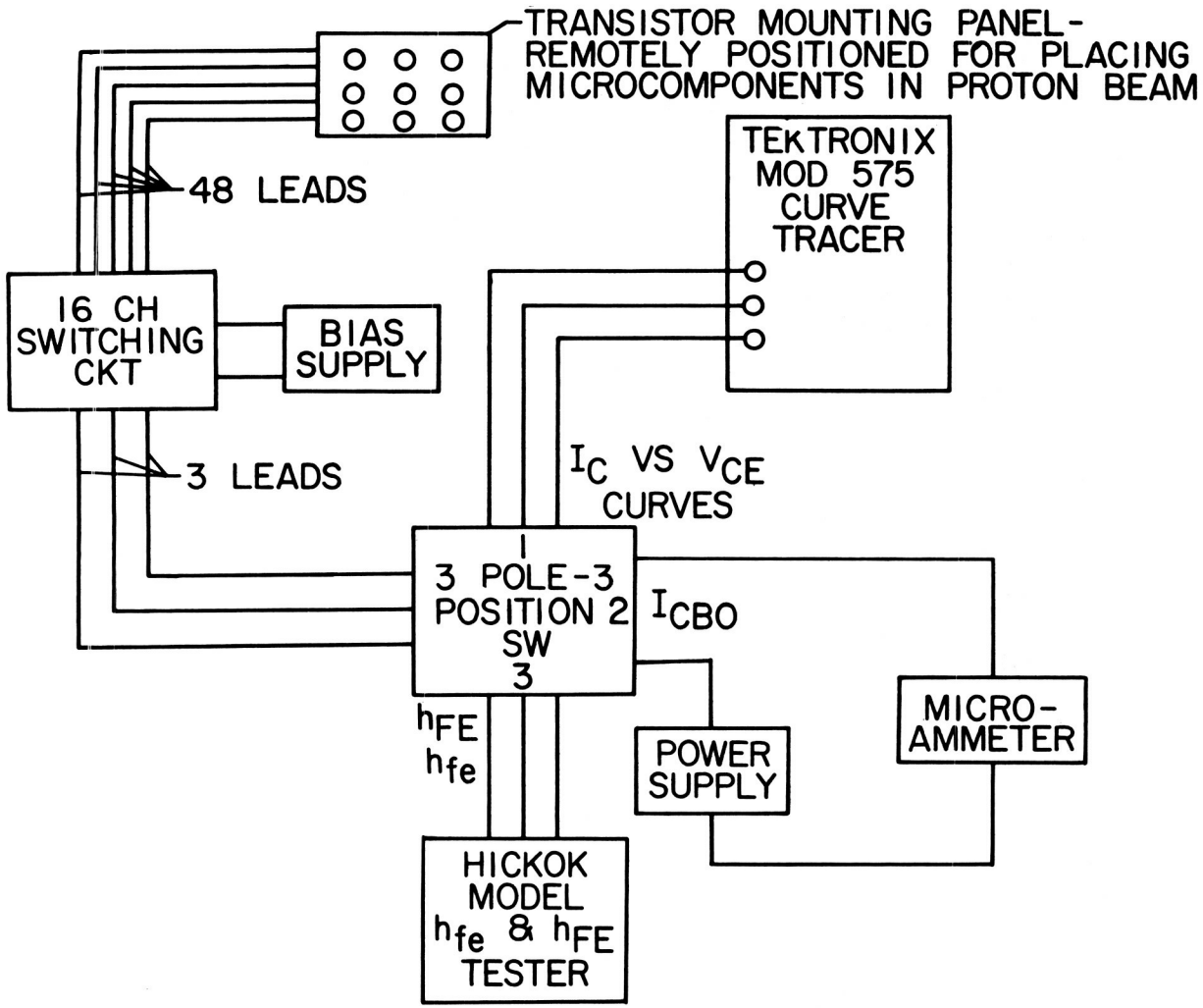

NASA

Figure 8.- Schematic of a typical experimental irradiation setup as used at Harvard and ORNL for bombardment with 128 Mev and 22 Mev protons, respectively.

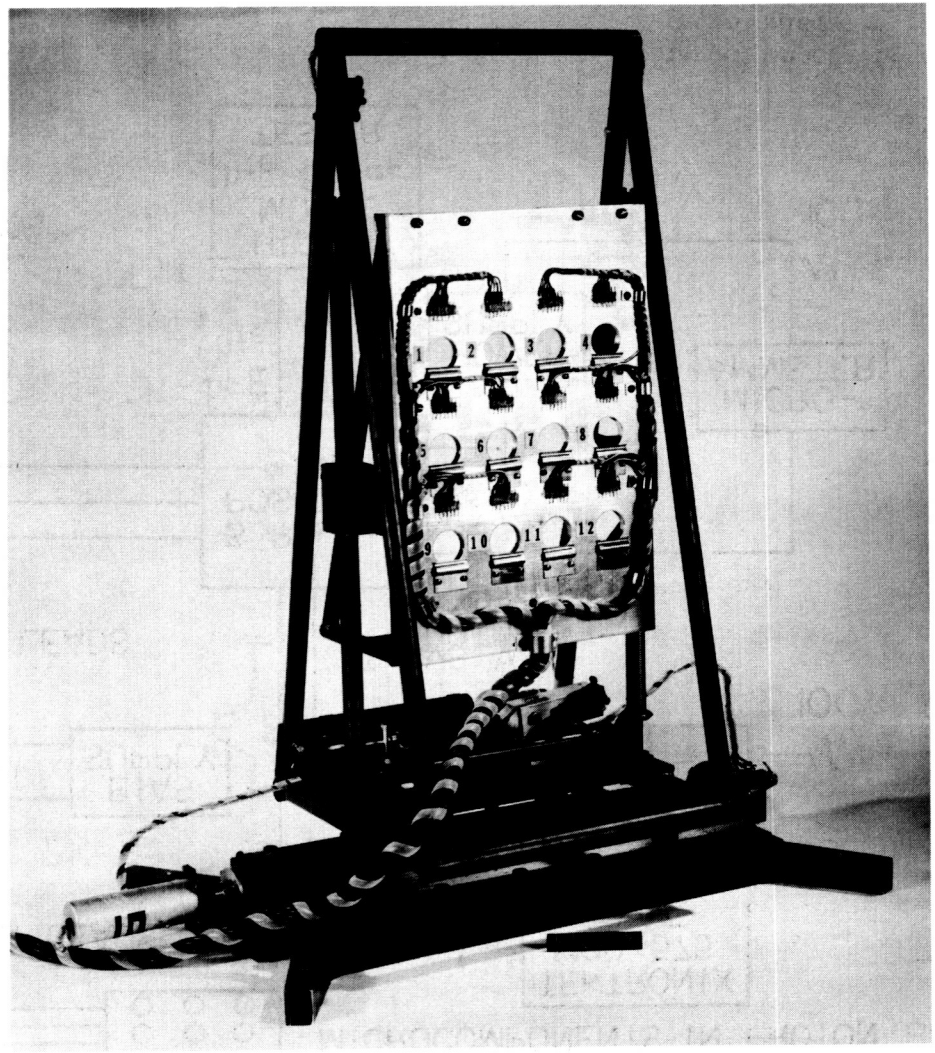

NASA

Figure 9.- Experimental setup showing remotely controlled target positioning carriage. Targets are centered in the numbered holes.

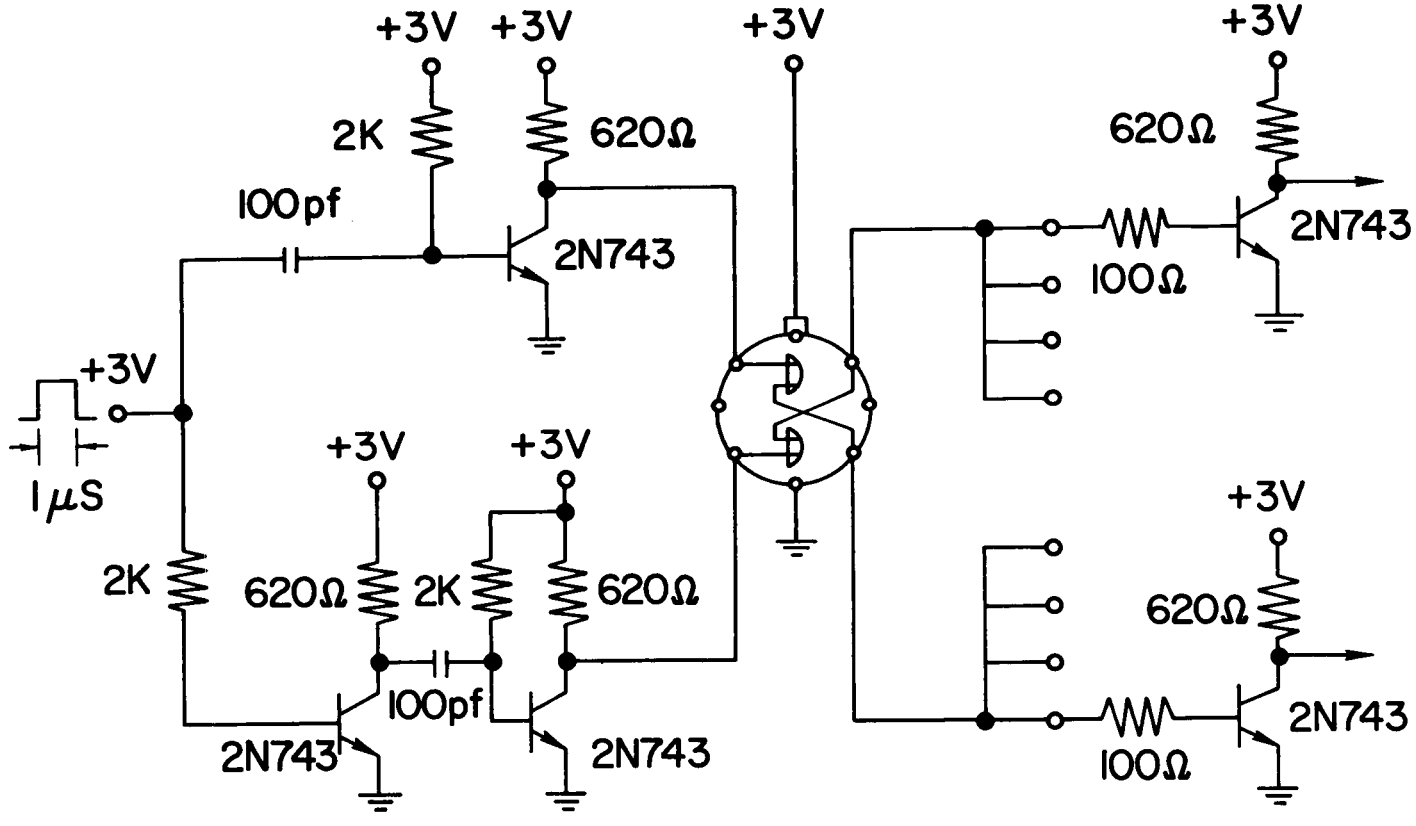

NASA

Figure 10.- Wiring diagram used for the experimental proton irradiation of the type "F" element. The circuit simulates micrologic inputs and loads.